ISSN 1063-7788, Physics of Atomic Nuclei, 2020, Vol. 83, No. 6, pp. 820–827. © Pleiades Publishing, Ltd., 2020.

NUCLEI
Theory

An Investigation on the Effects of Some Theoretical Models in the Cross-Section Calculations of ^{50,52,53,54}Cr(α, x) Reactions

H. Özdoğan[1)], M. Şekerci[2)], and A. Kaplan[2)*]

Received July 7, 2020; revised July 7, 2020; accepted July 7, 2020

Abstract—The probability of a nuclear reaction occurrence is defined as cross-section which can be obtained with the experimental studies or theoretical calculations. Theoretical calculations, in which various parameters and models are involved, are most commonly preferred way in the absence of experimental data or the existence of difficulties to perform an experiment. The cross-section calculation results are effected from the input parameters, which are directly related to the selected models. Thus, utilization of the most consistent model for an investigated reaction has an undeniable importance on the cross-section calculations. By considering this, the effects of level density models and alpha optical model potentials on the cross-section calculations of ^{50,52,53,54}Cr(α, x) reactions are investigated in this study. For calculations, TALYS code is used. Obtained calculation results of each investigated reaction are compared with the available experimental data, which are taken from the Experimental Nuclear Reaction Data (EXFOR) library.

DOI: 10.1134/S1063778820660060

1. INTRODUCTION

Many scientists from various branches have been working on finding a sustainable, clean, continuous, and efficient energy production method, which could be given as one of the most important problems of human beings for a long time. According to the reports, the energy consumption in the world has increased by almost 25% over the past few decades [1]. The energy dependent modern daily life and the growing world population show that this increase will continue in the future. One of the searches for a solution that can meet the enormous demand for energy, and perhaps the most promising one considering the benefits it provides in many areas, can be given as nuclear fusion technology. In addition to the possible contributions to technological and scientific development, the fact that it requires much less resources to be environmentally friendly, thanks to almost zero carbon emission level, and to produce equal amount of energy compared to traditional energy generation methods can be given as some examples of the advantages of this technology [2]. However, it is necessary to have a good scientific and technological background in many areas in order to manufacture and operate such devices that require complex technology and high level knowledge. In this context, studies related to structural material development and nuclear reaction mechanisms, which are among the many important areas that can be shown, are examples of important and contributing studies to the process. The reason of pointing these studies is due to their connection between the possibi- lities of sustainable operation of such a device which is directly connected to the convenient material selection in addition to having the knowledge of the effects of radiation on these materials [3–5]. For these purposes, experimental studies are generally carried out. However, in some cases, it may be not possible to perform an experimental study for a desired material, investigate the results of a nuclear reaction or study the effects of various parameters during the nuclear reaction processes. In such cases, it is also possible to use theoretical calculations performed with advanced computer codes such as TALYS, EMPIRE, etc., to have general and specific information about the examined situations or reactions [6–11]. There exist many outcomes of a nuclear reaction which may be useful to understand the nature of that reaction. One of such important outcomes is named as cross-section which simply identifies the probability of any reaction occurrence [12]. The motivation of this study is in this context and the main aim is to investigate the effects of two important parameters' effects on the nuclear reaction calculations for a known fusion structural material. Parameters such

[1)]Department of Medical Imaging Techniques, Vocational School of Health Services, Antalya Bilim University, Antalya, Turkey.
[2)]Department of Physics, Faculty of Arts and Sciences, Süleyman Demirel Universit, Isparta, Turkey.
[*]E-mail: abdullahkaplan@sdu.edu.tr

as level density models and alpha optical model potentials have a direct effect on the results of cross-section calculations [13–16]. Due to that, by considering the importance of these parameters on the cross-section calculations and the importance of the structural material development studies, this study is conducted. The effects of individual and simultaneous utilization of the level density models and the alpha optical model potentials on the cross-section calculations of (α, x) reactions for different isotopes of structural fusion material chromium are investigated in this study. Outcomes from examined reaction routes, which are $^{50}\mathrm{Cr}(\alpha,x)^{48}\mathrm{Cr}$, $^{50}\mathrm{Cr}(\alpha,x)^{49}\mathrm{Cr}$, $^{50}\mathrm{Cr}(\alpha,x)^{51}\mathrm{Cr}$, $^{52}\mathrm{Cr}(\alpha,x)^{54}\mathrm{Mn}$, $^{53}\mathrm{Cr}(\alpha,x)^{54}\mathrm{Mn}$, and $^{54}\mathrm{Cr}(\alpha,x)^{56}\mathrm{Mn}$, have been analyzed by using the experimental literature data taken from the Experimental Nuclear Reaction Data (EXFOR) library [17]. For this purpose, in addition to the graphical comparisons for each reaction, mean-weighted-deviation [18] calculations are also performed.

2. CALCULATION METHODS

In accordance with the aim and motivation of this study, effects of the level density models and the alpha optical model potentials on the crosssection calculations are investigated by using the TALYS v1.9 [19] code. TALYS is a compact and freely distributed code which could be used for various nuclear reaction calculations, such as crosssections, astrophysical reaction rates, medical isotope production yields, etc [19]. It is also possible to select among various models and numerous parameters from the TALYS code such as the level density models and the alpha optical model potentials, gamma-ray strength functions and etc. There exist six level density models available in the TALYS code, where three of them are phenomenological and three of them are microscopic. It is known that all phenomenological level density models are derived from the Fermi Gas Model (FGM) [20], in which the assumption of nucleons hold the lowest energy levels concept is accepted. In accordance with the acceptance in FGM, it is also possible that the nucleons could fill the higher energy levels upon an excitation. TALYS uses a phenomenological one, which is Constant Temperature + Fermi Gas Model (CT + FGM) [21, 22], as the default level density model in addition to the possibility of employing two other phenomenological level density models which are Back Shifted Fermi Gas Model (BSFGM) [23, 24] and Generalized Superfluid Model (GSM) [25, 26] according to the user's request. In addition to these phenomenological level density models, three microscopic level density model options are also available in the TALYS code, which are Skyrme Force–Goriely (SFG) [27], Skyrme Force–Hilaire (SFH) [28] and Gogny Force dependent (GFD) [29] models. All these microscopic level density model options of the TALYS code are developed by using the tabulated data from different studies and named in accordance with the researchers who performed these studies.

On the other hand, eight alpha optical model potential options are available in the TALYS code. The default one among them is named as normal alpha potential and developed with the Watanabe folding approach with Koning–Delaroche nucleon potentials [30]. Another one is derived from the results of McFadden and Satchler [31]'s study. This model is relatively old compared to the others. Three models are adopted from the study of Demetriou et al., [32] where two of them are included by using the propositions of two tables for the imaginary potential and the final one is introduced as dispersive model. Another alpha optical model potential of the TALYS code is derived from the particular study of Avrigeanu et al., [33], where all possible reaction channels of alphaparticle induced reactions on the nuclei of mass range $A \approx 45$–209 are examined to have better aspect of the interactions below Coulomb barrier. In addition to that one, one more model is derived from another study of Avrigeanu et al. [34]. Final possibility of alpha optical model potential of the TALYS code is implemented from the study of Nolte et al. [35]

In this study, the given steps are followed to achieve the desired goal of this study and to examine the effects of the mentioned quantities. As the first step, the alpha optical model potential was fixed to the default one of the TALYS code. Then, all available level density models are utilized separately for each investigated reaction. The results obtained by the calculations made in this way are compared with the experimental data and the most compatible level density model is determined for each reaction. In the second step, the level density model is fixed to the default one of the TALYS code and all available alpha optical model potentials are utilized separately for each investigated reaction. By doing so, the most compatible alpha optical model potential is found by comparing the obtained results with the experimental data. In the last step, the most compatible models found for each reaction are used together and the calculated results are compared with experimental data. In addition to graphical analysis, meanweighteddeviation calculation results are also used to compare the calculation results and the experimental data. Equation (1) [18] is used for the mean weighteddeviation calculations.

$$F = \left[\frac{1}{N}\sum_{i=1}^{N}\left[\left(\sigma_i^{\mathrm{calc}} - \sigma_i^{\mathrm{expr}}\right)/\Delta\sigma_i^{\mathrm{expr}}\right]^2\right]^{1/2}. \quad (1)$$

Table 1. Mean-weighted-deviation results of the level density model employed cross-section calculations

Reaction	TALYS 1.9 CT + FGM	TALYS 1.9 BSFGM	TALYS 1.9 GSM	TALYS 1.9 SFG	TALYS 1.9 SFH	TALYS 1.9 GFD
^{50}Cr$(\alpha,x)^{48}$Cr	13.915348	10.868692	9.105904	17.025712	12.577467	24.489108
^{50}Cr$(\alpha,x)^{49}$Cr	3.803705	3.754691	3.802726	9.569049	4.141237	3.985051
^{50}Cr$(\alpha,x)^{51}$Cr	2.646707	2.458637	2.562365	3.794249	2.844126	4.448310
^{52}Cr$(\alpha,x)^{54}$Mn	4.033824	3.585246	4.364153	3.697920	3.540993	3.748908
^{53}Cr$(\alpha,x)^{54}$Mn	3.293636	2.939527	4.323405	2.566778	2.450672	3.000257
^{54}Cr$(\alpha,x)^{56}$Mn	5.500638	4.275625	6.410066	4.402480	4.689563	6.498242
Total F values	33.193858	27.882418	30.568619	41.056188	30.244058	46.169876

The meanweighteddeviation calculation result, F, for N numbered data is a representation of the consistency between the calculated cross-section data, $\sigma_i^{\rm calc}$, and the experimental crosssection values, $\sigma_i^{\rm expr}$, which has an uncertainty, $\Delta\sigma_i^{\rm expr}$. The lower F values refer to a better consistency between the calculated and the experimental crosssection data.

3. RESULTS AND DISCUSSION

In this study, the effects of level density models and the alpha optical model potentials on the cross-section calculations of alpha particle induced reactions on several chromium isotopes are investigated. Graphical representations of the calculation results are given in Figs. 1–6 with the available experimental data. In addition, the mean-weighted-deviation calculation results can be seen in Tables 1–3.

The experimental data of Levkovskii [36] and theoretical calculation results for ^{50}Cr$(\alpha,x)^{48}$Cr reaction are presented in Fig. 1. As it can be seen from the numerical values of mean-weighted-deviation results given in Tables 1 and 2, the GSM and McFadden–Satchler could be pointed as the level density model and the alpha optical model potential that produced the most consistent results with the experimental data. On the other hand, as it can be seen from Fig. 1 and Table 3, their simultaneous utilization generated more consistent calculation results compared to their individual utilization.

In Fig. 2, calculation results for the ^{50}Cr$(\alpha,x)^{49}$Cr reaction are compared with the experimental data of Levkovskii [36] and Hermanne et al. [37]. Theoretical calculations resulted in good harmony with the experimental data. The BSFGM could be pointed as the most consistent level density model with the 3.754 mean-weighted-deviation result while McFadden and Satchler could be given as the one among all alpha optical model potentials by producing 3.747 mean-weighted-deviation result. Similar to the ^{50}Cr$(\alpha,\ x)^{48}$Cr reaction, simultaneous utilization of the pointed options generated more consistent calculation result supported by the mean-weighted-deviation result, 3.721.

The data from Levkovskii [36] are used for the comparison of the calculations obtained for the ^{50}Cr$(\alpha,\ x)^{51}$Cr reaction. Graphical representations given in Fig. 3 and the mean- weighted-deviation calculations point the BSFGM and the McFadden–Satchler as the most consistent level density model and the alpha optical model potential, whereas, the smallest F value is obtained if these two are utilized together.

The calculation results for the ^{52}Cr$(\alpha,\ x)^{54}$Mn reaction versus the data of Levkovskii [36] are represented in Fig. 4. Obtained calculations shaped similar geometries with the experimental data. The F values from the tables point the SFH and the Demetriou et al. [32]'s Table 2 as the most consistent options in the individual utilization. On the other hand, the simultaneous utilization generated more consistent results than the individual case.

The ^{53}Cr$(\alpha,x)^{54}$Mn reaction's calculations are compared with the data of Levkovskii [36] in Fig. 5. For this reaction, the SFH and the Demetriou et al. [32]'s Dispersive model could be pointed as the options which produced more compatible results with the experimental data. Likewise to the previous reactions, the simultaneous utilization produced better results with respect to the individual utilizations of the pointed options, as it can be seen from the Table 1–3.

Comparisons for the last investigated reaction of this study, which is ^{54}Cr$(\alpha,x)^{56}$Mn, are given in Fig. 6. As it can be seen, calculation results are able to generate similar shape with the data of Levkovskii [36]. For the individual utilization of the level density model and the alpha optical model potential options,

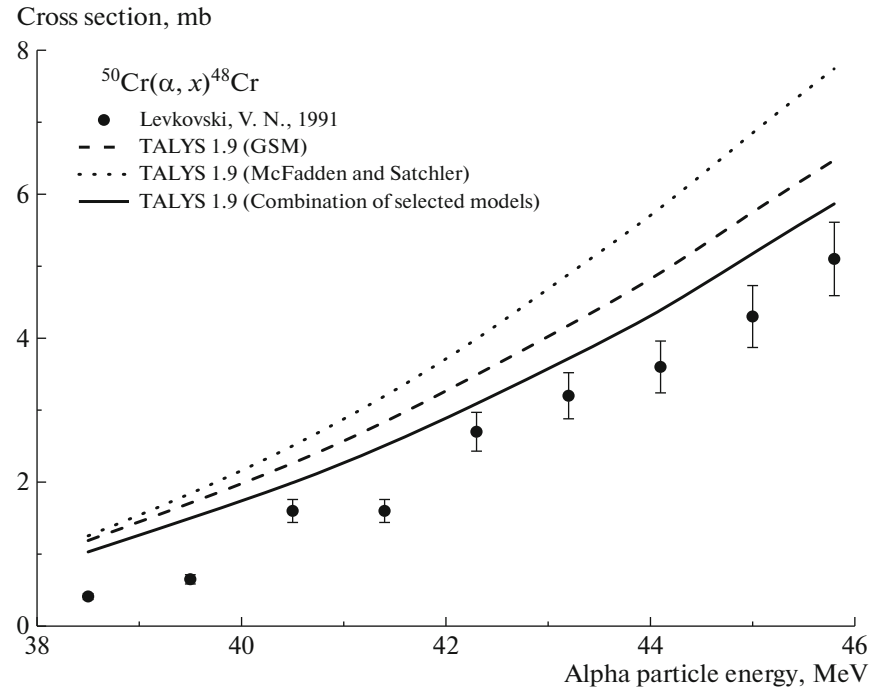

Fig. 1. Comparison of experimental data and theoretical calculation results for $^{50}\mathrm{Cr}(\alpha, x)^{48}\mathrm{Cr}$ reaction.

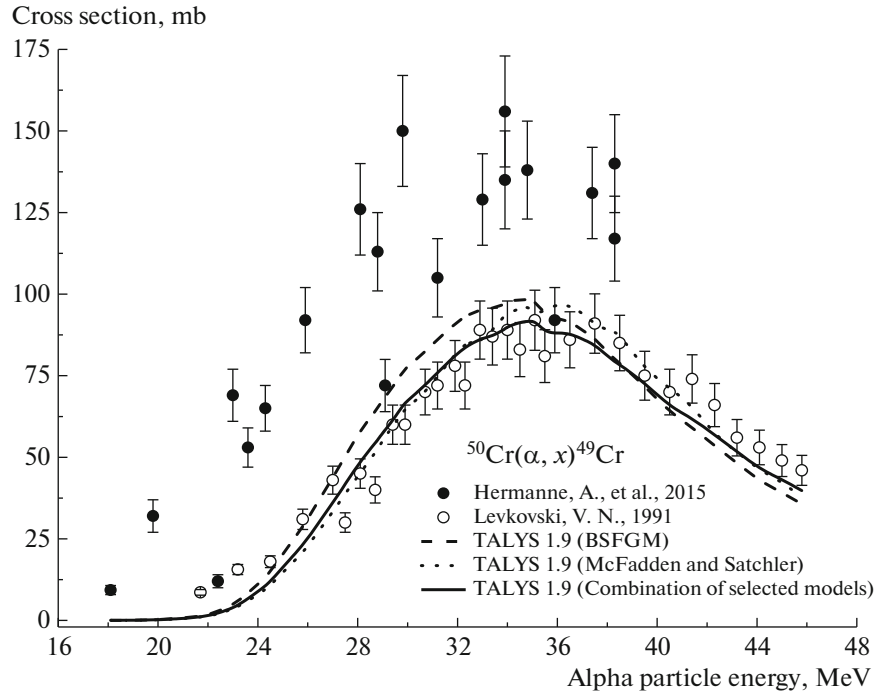

Fig. 2. Comparison of experimental data and theoretical calculation results for $^{50}\mathrm{Cr}(\alpha, x)^{49}\mathrm{Cr}$ reaction.

the BSFGM and the Nolte et al. [35] could be pointed as the most successful options. On the other hand, as it can be seen from Table 3, their simultaneous utilization generated more compatible results with the experimental data.

4. SUMMARY AND CONCLUSIONS

In this study, the cross-section calculations for the $^{50}\mathrm{Cr}(\alpha, x)^{48}\mathrm{Cr}$, $^{50}\mathrm{Cr}(\alpha, x)^{49}\mathrm{Cr}$, $^{50}\mathrm{Cr}(\alpha, x)^{51}\mathrm{Cr}$, $^{52}\mathrm{Cr}(\alpha, x)^{54}\mathrm{Mn}$, $^{53}\mathrm{Cr}(\alpha, x)^{54}\mathrm{Mn}$, and $^{54}\mathrm{Cr}(\alpha, x)^{56}\mathrm{Mn}$ reactions by using the level density models and alpha

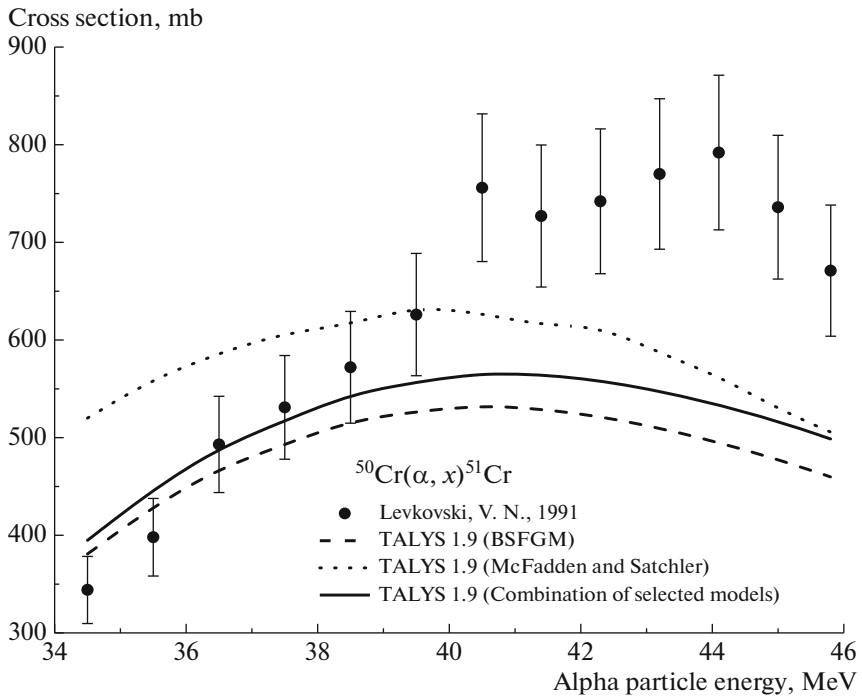

Fig. 3. Comparison of experimental data and theoretical calculation results for $^{50}\mathrm{Cr}(\alpha, x)^{51}\mathrm{Cr}$ reaction.

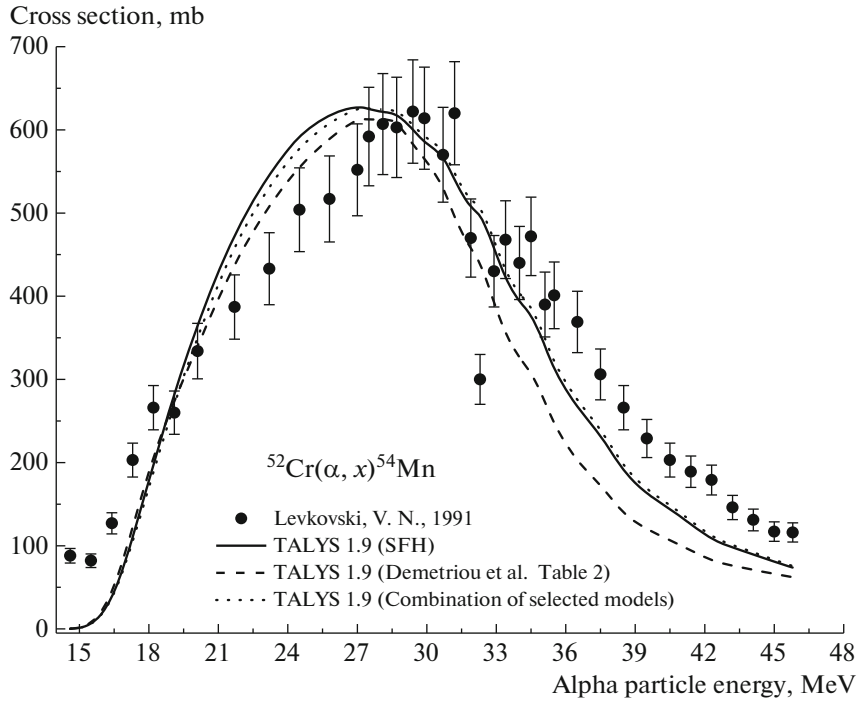

Fig. 4. Comparison of experimental data and theoretical calculation results for $^{52}\mathrm{Cr}(\alpha, x)^{54}\mathrm{Mn}$ reaction.

optical model potentials are investigated. Obtained finding and interpretations with respect to them could be given as,

1. Considering the obtained results for all investigated reactions in this study, the default level density model and the default alpha optical model potential options failed to produce the most compatible calculation results with the experimental data. Thus, it may be tried to

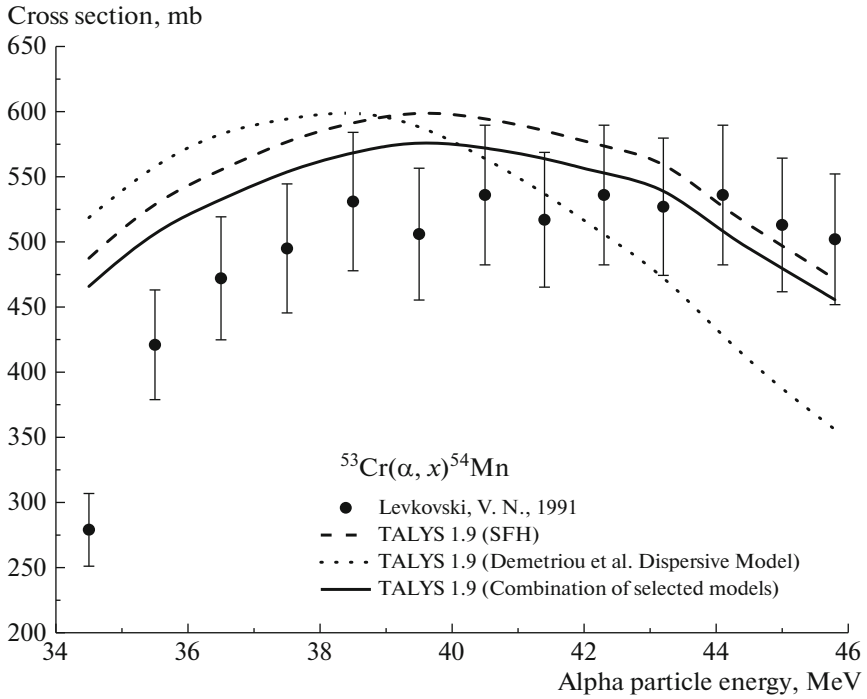

Fig. 5. Comparison of experimental data and theoretical calculation results for $^{53}\mathrm{Cr}(\alpha, x)^{54}\mathrm{Mn}$ reaction.

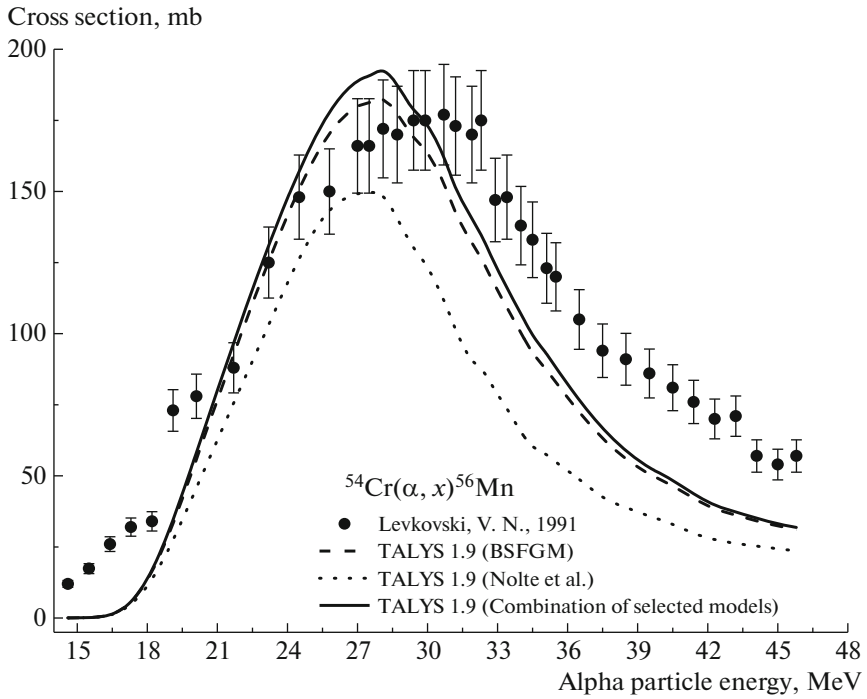

Fig. 6. Comparison of experimental data and theoretical calculation results for $^{54}\mathrm{Cr}(\alpha, x)^{56}\mathrm{Mn}$ reaction.

optimize the parameters of these models for the investigated reactions in this study.

2. For all reactions examined in this study, the calculations results most compatible with the experimental data are obtained in the case of utilizing the most consistent level density and alpha optical model potential simultaneously. This situation is also recognizable from the figures and the tables.

3. Considering the outcome given in the previous

Table 2. Mean-weighted-deviation results of the alpha optical model potential employed cross-section calculations

Reaction	TALYS 1.9 Normal Alpha Optical	TALYS 1.9 McFadden and Satchler	TALYS 1.9 Demetriou et al. Table 1	TALYS 1.9 Demetriou et al. Table 2	TALYS 1.9 Demetriou et al. Dispersive Model	TALYS 1.9 Avrigeanu et al. [29]	TALYS 1.9 Nolte et al.	TALYS 1.9 Avrigeanu et al. [30]
$^{50}Cr(\alpha,x)^{48}Cr$	13.882970	10.684137	12.150743	12.880813	12.386187	13.915348	28.176079	23.877481
$^{50}Cr(\alpha,x)^{49}Cr$	3.769279	3.747187	3.766115	3.868008	3.792832	3.803705	8.071519	6.153204
$^{50}Cr(\alpha,x)^{51}Cr$	2.591650	2.561393	2.586437	2.621241	2.573813	2.646707	2.711410	2.658747
$^{52}Cr(\alpha,x)^{54}Mn$	4.000532	3.989528	4.006574	3.975510	4.076171	4.033824	4.049281	4.035638
$^{53}Cr(\alpha,x)^{54}Mn$	3.303444	3.338823	3.265055	3.449532	3.032048	3.293636	3.414623	3.320209
$^{54}Cr(\alpha,x)^{56}Mn$	5.496267	5.506394	5.500909	5.473082	5.560703	5.500638	5.394187	5.460279
Total F values	33.044142	29.827462	31.275833	32.268186	31.421754	33.193858	51.817099	45.505558

Table 3. Mean-weighted-deviation results of the determined most consistent level density models and alpha optical model potentials in addition to their jointly use

Reaction	TALYS 1.9 Selected level density model	TALYS 1.9 Selected alpha optical model	TALYS 1.9 Combination of selected models
$^{50}Cr(\alpha,x)^{48}Cr$	9.105904	10.684137	7.064337
$^{50}Cr(\alpha,x)^{49}Cr$	3.754691	3.747187	3.721691
$^{50}Cr(\alpha,x)^{51}Cr$	2.458637	2.561393	2.095007
$^{52}Cr(\alpha,x)^{54}Mn$	3.540993	3.975510	3.489834
$^{53}Cr(\alpha,x)^{54}Mn$	2.450672	3.032048	2.112967
$^{54}Cr(\alpha,x)^{56}Mn$	4.275625	5.394187	4.155398

item, it can be speculated that the level density models and alpha optical model potentials should be used together in order to evaluate more optimal and consistent theoretical cross-section calculations. This instance should be seriously taken into account and investigated by performing many calculations for various reactions.

4. As it can be seen from the total lines given in Tables 1 and 2, the BSFGM and the McFadden and Satchler have the lowest overall mean-weighted-deviation calculation results for the investigated reactions in this paper.

5. More detailed studies by using various parameters of the TALYS code for the level density models such as the explicit collective enhancement of the level densities, damping of the collective effects in the effective level densities or vibrational enhancement of the level densities should be conducted to see their effects on the investigated reactions.

6. Similarly, various alpha optical model potential related parameter effects, such as normalization factor for the shape of the double-folding alpha potential or normalization factor for the depth of the double-folding alpha potential, should be conducted for detailed investigations on alpha optical model potential effects on the investigated reactions. To contribute more effectively on the theoretical model development studies, similar studies should be conducted for many reactions. By doing so, significant contribution may be provided to the literature which could be beneficial for the further studies.

REFERENCES

1. *World Energy Outlook 2018* (International Energy Agency, Vienna, 2018).

2. E. E. Bloom, S. J. Zinkle, and F. W. Wiffen, J. Nucl. Mater. **329–333**, 12 (2004).
3. K. Ehrlich, Phil. Trans. R. Soc. London, Ser. A **357**, 595 (1999).
4. M. Victoria, N. Baluc, and P. Spätig, Nucl. Fusion **41**, 1047 (2001).
5. P. M. Raole, S. P. Deshpande, and DEMO Team, Trans. Indian Inst. Met. **62**, 105 (2009).
6. A. Azzam, S. A. Said, and M. Al-abyad, Appl. Radiat. Isot. **91**, 109 (2014).
7. A. H. M. Solieman, M. Al-Abyad, F. Ditroi, and Z. A. Saleh, Nucl. Instrum. Methods Phys. Res., Sect. B **366**, 19 (2016).
8. E. Vagena and S. Stoulos, Nucl. Phys. A **957**, 259 (2017).
9. S. Stoulos and E. Vagena, Nucl. Phys. A **980**, 1 (2018).
10. S. Parashari, S. Mukherjee, V. Vansola, R. Makwana, N. L. Singh, and B. Pandey, Appl. Radiat. Isot. **133**, 31 (2018).
11. W. Ali, M. Tashfeen, and M. Hussain, Appl. Radiat. Isot. **144**, 124 (2019).
12. G. R. Satchler, *Introduction to Nuclear Reactions* (McMillan, London, 1980).
13. H. Özdoğan, M. Şekerci, A. Kaplan, and H. Sarpün, Appl. Radiat. Isot. **140**, 29 (2018).
14. H. Özdoğan, M. Şekerci, and A. Kaplan, Appl. Radiat. Isot. **143**, 6 (2019).
15. M. Şekerci, H. Özdoğan, and A. Kaplan, Radiochim. Acta **108**, 11 (2020).
16. M. Şekerci, Radiochim. Acta **108**, 459 (2020).
17. V. V. Zerkin and B. Pritychenko, Nucl. Instrum. Methods Phys. Res., Sect. A **888**, 31 (2018).
18. V. P. Lunev, Y. N. Shubin, and N. V. Kurenkov, Appl. Radiat. Isot. **50**, 541 (1999).
19. A. Koning, S. Hilaire, and S. Goriely, *TALYS-1.9 A Nuclear Reaction Program, User Manual,* 1st ed. (Netherlands, 2017). https://tendl.web.psi.ch/tendl_2019/talys.html.
20. E. Fermi, Z. Phys. **36**, 902 (1926).
21. A. Gilbert and A. G. W. Cameron, Can. J. Phys. **43**, 1446 (1965).
22. A. V. Ignatyuk, K. K. Istekov, and G. N. Smirenkin, Sov. J. Nucl. Phys. **29**, 450 (1979).
23. H. Baba, Nucl. Phys. A **159**, 625 (1970).
24. W. Dilg, W. Schantl, H. Vonach, and M. Uhl, Nucl. Phys. A **217**, 269 (1973).
25. A. V. Ignatyuk, G. N. Smirenkin, and A. S. Tishin, Sov. J. Nucl. Phys. **21**, 255 (1975).
26. A. J. Koning, S. Hilaire, and S. Goriely, Nucl. Phys. A **810**, 13 (2008).
27. S. Goriely, S. Hilaire, and A. J. Koning, Phys. Rev. C **78**, 064307 (2008).
28. S. Hilaire and S. Goriely, Nucl. Phys. A **779**, 63 (2006).
29. S. Hilaire, M. Girod, S. Goriely, and A. J. Koning, Phys. Rev. C **86**, 064317 (2012).
30. A. J. Koning and J. P. Delaroche, Nucl. Phys. A **713**, 231 (2003).
31. L. McFadden and G. R. Satchler, Nucl. Phys. **84**, 177 (1966).
32. P. Demetriou, C. Grama, and S. Goriely, Nucl. Phys. A **707**, 253 (2002).
33. V. Avrigeanu, M. Avrigeanu, and C. Mănăilescu, Phys. Rev. C **90**, 044612 (2014).
34. V. Avrigeanu, P. E. Hodgson, and M. Avrigeanu, Phys. Rev. C **49**, 2136 (1994).
35. M. Nolte, H. Machner, and J. Bojowald, Phys. Rev. C **36**, 1312 (1987).
36. V. N. Levkovskii, *Activation Cross Sections for the Nuclides of Medium Mass Region* ($A = 40–100$) *with Medium Energy* ($E = 10–50$ *MeV) Protons and Alpha-Particles (Experiment and Systematics)* (Inter-Vesti, Moscow, 1991) [in Russian].
37. A. Hermanne, R. A. Rebeles, F. Tárkányi, and S. Takács, Nucl. Instrum. Methods Phys. Res., Sect. B **356–357**, 28 (2015).